

Cite this: *Dalton Trans.*, 2018, **47**, 17304

# Thermal dehydrochlorination in the 4-fluoroaniline–trichloroborane system: identification of reactive intermediates involved in the formation of *B,B',B''*-trichloro-*N,N',N''*-tri((4-fluoro)phenyl)borazine†

Jennifer Hahn,<sup>a</sup> Matthias Krieg,<sup>a</sup> Constanze Keck,<sup>a</sup> Căcilia Maichle-Mössmer,<sup>b</sup> Reinhold F. Fink<sup>c</sup> and Holger F. Bettinger<sup>id</sup> \*<sup>a</sup>

Borazines are used in chemical vapor deposition processes to produce hybrid graphene–boron nitride nanostructures. As the knowledge on the mechanism of borazine formation is scarce, we studied the mechanism of formation of *B,B',B''*-trichloro-*N,N',N''*-tri(*p*-fluorophenyl)borazine (**3a**) from *p*-fluoroaniline and boron trichloride employing NMR spectroscopy, X-ray single crystal structure analysis, trapping experiments, and computational chemistry methods up to the coupled cluster CCSD(T) level of theory. These studies suggest the initial formation of the 1 : 1 adduct **1a** (ArNH<sub>2</sub>BCl<sub>3</sub>, Ar = 4-fluorophenyl) with a dative B–N bond that could be fully characterized including single crystal X-ray diffraction. Adduct **1a** undergoes unimolecular hydrogen chloride elimination with a first-order rate constant of  $k_1 = 3.03(7) \times 10^{-2} \text{ min}^{-1}$  in toluene at 100 °C. This rate constant is in very good agreement with the one derived ( $k_1 = 3.18 \times 10^{-2} \text{ min}^{-1}$ ) from computed activation parameters ( $\Delta H^\ddagger_{373,15} = 28.1 \text{ kcal mol}^{-1}$ ,  $\Delta S^\ddagger_{373,15} = 1.56 \text{ eu}$ ,  $\Delta G^\ddagger_{373,15} = 27.6 \text{ kcal mol}^{-1}$ ). The product of the first hydrogen chloride evolution is anilindichloroborane ArNHBCl<sub>2</sub> (**2a**). Compound **2a** cannot be isolated in a pure form due to instability, but its presence as a transient reactive intermediate can be derived from NMR spectroscopy. Reactive intermediates other than anilindichloroborane cannot be assigned by NMR spectroscopy. We propose that the mechanism of formation of borazine **3a** involves the reaction of **2a** with 4-fluoroaniline as the rate determining step.

Received 1st October 2018,  
Accepted 2nd November 2018

DOI: 10.1039/c8dt03954b

rsc.li/dalton

## Introduction

Band gap engineering of graphene and nanographene molecules by selective doping with boron and nitrogen units is an important topic in materials science today.<sup>1–23</sup> Most of the techniques available for single layered systems rely on CVD processes for producing BN-graphene from gaseous boron, nitrogen, and carbon precursors.<sup>2,24–26</sup> Promising starting materials include borazines<sup>27</sup> as they offer options to incorporate all the needed atoms (B, N, C) in one molecule and in a precise ratio

that can be adjusted through the substitution pattern around the borazine core. The synthesis of borazines is known for a long time and methods for their assembly have not significantly changed since the discovery of borazine in 1926.<sup>28</sup> Carbon-rich borazines are mostly synthesized *via* the reaction of boron trichloride with amines/anilines to form the corresponding *B,B',B''*-trichloro-*N,N',N''*-triorganylborazines that are subjected to nucleophilic reactions with organometallic compounds afterwards.<sup>29</sup> There are two different ways to synthesize these borazines: a base (in most cases triethylamine) assisted<sup>30</sup> and a thermal route. The thermal reaction, which was first observed in 1889 by Rideal<sup>31</sup> and recognized to yield borazine by Jones and Kinney<sup>32</sup> in 1939, can further be divided into two subgroups of reactions that either use free amines and boron trichloride<sup>29,32</sup> or ammonium tetrachloroborates<sup>33–35</sup> as the starting materials.

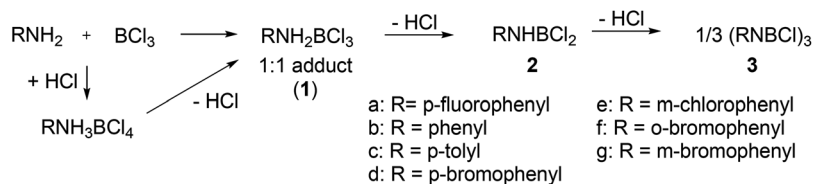
Although the synthetic strategy *via* *B,B',B''*-trichloroborazines is widely employed for the synthesis of hexaarylborazines,<sup>11,36,37</sup> the available knowledge about reactive intermediates is scarce. Most mechanistic suggestions were made on the basis of the kinetics of hydrogen chloride evolution<sup>29</sup> or

<sup>a</sup>Institut für Organische Chemie, Universität Tübingen, Auf der Morgenstelle 18, 72076 Tübingen, Germany. E-mail: Holger.Bettinger@uni-tuebingen.de; Fax: +49 7071/29-5244

<sup>b</sup>Institut für Anorganische Chemie, Universität Tübingen, Auf der Morgenstelle 18, 72076 Tübingen, Germany

<sup>c</sup>Institut für Physikalische und Theoretische Chemie, Universität Tübingen, Auf der Morgenstelle 18, 72076 Tübingen, Germany

† Electronic supplementary information (ESI) available. CCDC 1535682, 1535683 and 1590012. For ESI and crystallographic data in CIF or other electronic format see DOI: 10.1039/c8dt03954b



**Scheme 1** Simple reaction sequence from amine and boron trichloride to *B,B',B''*-trichloroborazine.

the formation of isolated intermediates.<sup>38</sup> The general reaction sequence (Scheme 1) that proceeds *via* subsequent elimination of hydrogen chloride has been recognized to be “oversimplified”.<sup>30</sup> For example, the chemical composition of the precipitate formed upon reaction of amine and boron trichloride, tetraammonium tetrachloroborate or a 1 : 1 adduct (**1**) depends on the substituent R.<sup>39</sup> The aminodichloroborane **2** could not be identified so far as a reactive intermediate *en route* to borazine **3**. If it can be isolated, then it is isolated only with *o,o'*-disubstituted aryl groups, but these derivatives cannot be transformed into **3** subsequently.<sup>40</sup>

The closely related reaction of ammonia and boron trichloride has received some attention due to its importance for the production of boron nitride under CVD conditions.<sup>41–45</sup> The datively bonded 1 : 1 adduct,  $\text{BCl}_3\text{NH}_3$ , could be first characterized by matrix isolation techniques<sup>46</sup> and later on also by single crystal X-ray analysis.<sup>47</sup> Kinetic investigations of the gas-phase reaction have shown that the first elimination of hydrogen chloride to give aminodichloroborane is facile,<sup>42,43</sup> with a barrier of 8.4 kcal mol<sup>-1</sup> with respect to the energy of  $\text{NH}_3$  and  $\text{BCl}_3$ .<sup>43</sup> Further steps involve the reaction of aminodichloroborane with an excess of ammonia ( $\text{BCl}_2\text{NH}_2 + \text{NH}_3 \rightarrow \text{BCl}(\text{NH}_2)_2 + \text{HCl}$ , a barrier of 18.5 kcal mol<sup>-1</sup>), but also surface reactions have been identified to be important.<sup>43</sup>

A better understanding of the species participating in the formation of *B,B',B''*-trichloroborazines in solution phase reactions is certainly important for the optimization of the reaction conditions and for gaining access to more complex starting materials for CVD processes. In view of the limited knowledge, we decided to study the aniline–trichloroborane system and some aspects of its thermal dehydrochlorination. We here report our investigation of the reaction of trichloroborane with 4-fluoroaniline (Scheme 1, R = 4-fluorophenyl). The choice of 4-fluoroaniline was motivated by the favorable properties of the <sup>19</sup>F nucleus in NMR spectroscopy. In contrast to <sup>11</sup>B, <sup>19</sup>F NMR spectroscopy has a broad spectral range, usually yields sharp signals, and allows faster measurements, which is important for kinetic studies. It should be recognized that the fluorine substituent will influence the nucleophilicity of the aniline nitrogen and therefore the conclusions may not be general, but limited to this particular system. The basicity of 4-fluoroaniline ( $\text{p}K_s = 4.65$ ) is, however, similar to that of the parent aniline ( $\text{p}K_s = 4.87$ ).<sup>48</sup> Our study shows that the two reactants form a Lewis acid–base pair that undergoes a first order dehydrochlorination reaction to give the monomeric 4-(fluorophenyl)aminodichloroborane.

## Results

### The 1 : 1 adduct (**1**)

The addition of aromatic amines ( $\text{ArNH}_2$ ) to boron trichloride usually results in the formation of solids. Their composition depends on the aryl moiety and can either have the stoichiometry of a 1 : 1 complex (**1**,  $\text{ArNH}_2\text{BCl}_3$ ) or sometimes (*e.g.* Ar = *meta*-tolyl) that of an ammonium tetrachloroborate ( $\text{ArNH}_3\text{BCl}_4$ ).<sup>39</sup> The constitution of some of the 1 : 1 complexes was described as  $(\text{ArNHBCl}_2)\text{-HCl}$  based on IR spectroscopy and chemical behavior.<sup>39</sup> This proposal was later refuted in favor of a classical Lewis acid–base (dative) structure based on <sup>1</sup>H NMR and IR spectral data.<sup>49</sup>

The dropwise addition of a solution of 4-fluoroaniline in toluene to a toluene solution of boron trichloride at 0 °C produces a solid compound. The elemental analysis of the solid isolated by filtration shows it to be a 1 : 1 complex. The isolated solid 1 : 1 adduct shows no decomposition when stored for months at room temperature. The stability of such adducts has already been recognized by Blackborow *et al.*<sup>49,50</sup> Its constitution can be elucidated by spectroscopy. Diffuse reflectance infrared Fourier transform spectroscopy (DRIFTS) of the solid shows two signals at 3190 cm<sup>-1</sup> and 3174 cm<sup>-1</sup> that can be assigned to symmetric and asymmetric NH stretching vibrations, respectively, similar to earlier data reported by Blackborow and Lockhart.<sup>49</sup> The <sup>11</sup>B{<sup>1</sup>H} solid state NMR spectrum shows only one signal at 6.1 ppm, suggesting the presence of a tetracoordinate boron atom. The 1 : 1 complex shows sufficient solubility in benzene and dichloromethane to allow solution phase NMR spectroscopy. Its <sup>11</sup>B NMR chemical shift in  $[D]_6$ -benzene is 6.5 ppm. Compared to the isotropic chemical shift in the solid state the difference is very low (0.4 ppm), indicative of no fundamental structural differences between the solid and solution phases. In addition, an intensity ratio of 4 : 2 is observed in the <sup>1</sup>H NMR spectrum for the aromatic protons and the NH<sub>2</sub> group.

Further evidence for the constitution of the precipitate is gained from single crystal X-ray structural analysis. Adduct **1a** crystallizes in the orthorhombic system, space group *Pca*21 and *Z* = 4. Its molecular structure is shown in Fig. 1. All B–Cl bonds have equal lengths of 1.84 Å. They are longer than in free planar  $\text{BCl}_3$  (1.72–1.74 Å).<sup>51</sup> The coordination of chlorine around the boron atom is no longer planar, but tetrahedrally distorted with Cl–B–Cl angles of around 111°. The B–N bond has a length of 1.61 Å. The structure indicates a classic dative bonding in the 1 : 1 complex **1a**.<sup>47,52,53</sup> To our knowledge, this is

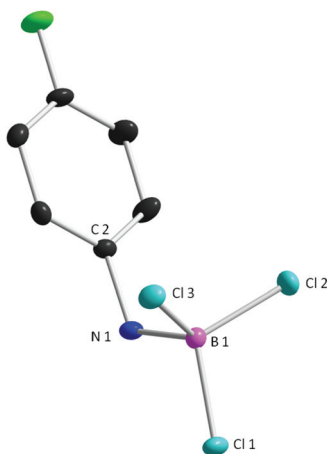


**Fig. 1** The molecular structure of the 1 : 1 complex **1a** in the solid state; selected bond lengths (in Å) and bond angles (in °): N1–B1 1.607(4), B1–Cl1 1.835(3), B1–Cl2 1.836(3), B1–Cl3 1.836(3); C2–N1–B1 117.7(2), Cl1–B1–Cl2 111.1(2), Cl1–B1–Cl3 110.8(2), Cl1–B1–N1 109.3(2), Cl2–B1–Cl3 111.4(2), Cl2–B1–N1 105.1(2), Cl3–B1–N1 108.9(2). Hydrogen atoms omitted for clarity.

the first structural characterization of a 1 : 1 complex formed between an aromatic amine and boron trichloride.

#### Composition of the reaction mixture before heating and the properties of the 1 : 1 complex (**1a**)

We investigated by  $^{11}\text{B}$  NMR spectroscopy also the mother liquors after separation of the initially formed solid 1 : 1 adduct. The signal at 6.5 ppm shows that the 1 : 1 complex is not fully precipitating initially and, upon standing, a further crop of 1 : 1 adduct crystallizes from the mother liquors. In addition, roughly 5% of borazine **3a** can be detected by  $^{11}\text{B}$  NMR. The initial formation of borazine during addition of aniline and boron trichloride in cold solutions has already been reported by Gerrard and Mooney.<sup>39</sup> Monitoring a benzene solution of the isolated 1 : 1 adduct **1a** kept at room temperature by  $^{19}\text{F}\{^1\text{H}\}$  NMR spectroscopy revealed only minor decomposition due to the formation of anilindichloroborane **2a** (see below for the assignment) after a period of three days. Importantly, no borazine formation was observed during this time. Likewise, stirring the mixture obtained after the addition of 4-fluoroaniline to boron trichloride at 0 °C does not change the amount of borazine. These experiments show that the initial borazine formation does not result from fast decomposition of **1a** and ceases once the addition of the components is completed.

To better understand the initial formation of borazine and the possible involvement of the 1 : 1 complex **1a**, additional experiments were performed. Heating the suspension of the 1 : 1 adduct in toluene until complete dissolution followed by quickly cooling to room temperature allows almost quantitative recovery of the precipitated 1 : 1 adduct **1a** as no significant changes in NMR spectra are observed. This is in agreement with the observation of Bartlett *et al.* that dissolution of adducts in toluene is faster than hydrogen chloride evol-

ution.<sup>38</sup> Addition of five equivalents of boron trichloride to the isolated complex **1a** does not result in any reaction over a period of one day at room temperature. Addition of five equivalents of 4-fluoroaniline to a solution of isolated **1a** at RT quickly produces a thick suspension. Two new products were observed in the reaction mixture. One is assigned to tri-(4-fluoroanilino)borane,  $\text{B}(\text{NHC}_6\text{H}_4\text{F})_3$  (**4a**), by comparison with NMR data that were obtained from a sample that we synthesized independently *via* aminolysis of  $\text{B}(\text{NMe}_2)_3$  with 4-fluoroaniline as described by Nöth *et al.* for trianilino-borane.<sup>54</sup> Compound **4a** is poorly soluble in benzene, but could be completely characterized by  $^1\text{H}$ ,  $^{13}\text{C}$ ,  $^{11}\text{B}$ , and  $^{19}\text{F}$  NMR spectroscopy. From the benzene solution, crystals could be grown that were of sufficient quality for single crystal X-ray analysis (Fig. 2). Compound **4a** crystallizes in the triclinic system, space group  $P\bar{1}$  with  $Z = 2$ . The BN bonds in **4a** have similar lengths (1.428, 1.435 and 1.438 Å), while for trianilino-borane two shorter and one significantly longer BN bond were reported (1.428, 1.431 and 1.442 Å).<sup>54</sup> The sum of the bond angles around the boron atom is 360°, confirming the expected trigonal-planar coordination. We also determined a solid state  $^{11}\text{B}$  NMR spectrum of **4a** and obtained an isotropic shift of 23.5 ppm that is virtually identical to that measured in benzene solution (23.5 ppm), indicating that the molecular structures in the solid state and those in solution are comparable.

The other product **5a** observed in the mixture obtained from the reaction of **1a** with five equivalents of 4-fluoroaniline has NMR spectral properties similar to but distinct from **4a**. In

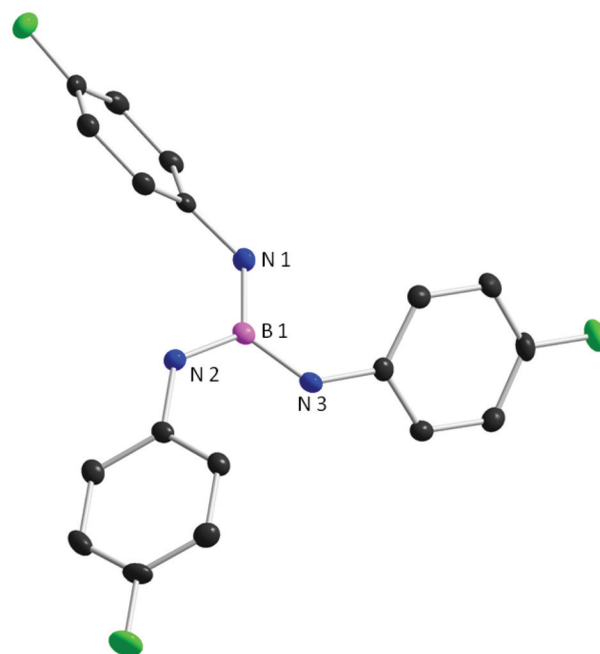


**Fig. 2** The molecular structure of tri-(4-fluoroanilino)borane **4a**; selected bond lengths (in Å) and bond angles (in °): N1–B1 1.435(2), N2–B1 1.438(2), N3–B1 1.428(2); N1–B1–N2 119.5(1), N1–B1–N3 120.4(1), N2–B1–N3 120.0(1). Hydrogen atoms omitted for clarity.

the  $^{19}\text{F}$  and  $^{11}\text{B}$  NMR the corresponding signals are shifted downfield ( $^{19}\text{F}$ :  $-120.1$  ppm vs.  $-122.7$  ppm;  $^{11}\text{B}$ :  $26.3$  ppm vs.  $23.5$  ppm), and the H(N) signal in the  $^1\text{H}$  NMR is also shifted downfield ( $4.60$  ppm vs.  $4.14$  ppm). Based on these slight shifts the product is identified as di-(4-fluoroanilino)chloroborane  $\text{ClB}(\text{NHC}_6\text{H}_4\text{F})_2$  (**5a**). The downfield shifts of  $2.7$  ppm in the  $^{19}\text{F}$  and  $2.9$  ppm in the  $^{11}\text{B}$  NMR are in agreement with computations ( $\Delta\delta(^{19}\text{F}) = 4.0$  ppm and  $\Delta\delta(^{11}\text{B}) = 3.9$  at the KT3/pcS-3//SCS-MP2/cc-pVTZ level of theory). Upon addition of two equivalents of 4-fluoroaniline to **1a**, compound **5a** is the only product and can be isolated. In the  $^1\text{H}$  NMR the H(N) proton and aromatic protons integrate in the required 1:4 ratio. As compound **5a** does not sublime without decomposition, a high resolution EI-MS spectrum could not be obtained, but the detection of a signal at  $m/z = 36.1$  (HCl) is supportive of the assignment to  $\text{ClB}(\text{NHC}_6\text{H}_4\text{F})_2$ .

We then varied the ratio of 4-fluoroaniline and boron trichloride in the initial addition at  $0^\circ\text{C}$ . As expected, a ten-fold excess of 4-fluoroaniline results in the formation of tri-(4-fluoroanilino)borane **4a**. On the other hand, a ten-fold excess of boron trichloride produces a significantly larger amount (roughly 13%) of borazine **3a**. Subsequent stirring of this reaction mixture does not increase the amount of borazine. This observation is supportive of the above statement that borazine formation ceases after the addition of components is completed. Hence, there must exist pathways to borazine that are only accessible as long as complex formation is not completed. As complex **1a** does neither react with an excess of 4-fluoroaniline nor react with boron trichloride to borazine, we conclude that once the formation of **1a** is completed, borazine formation will come to a halt. The actual mechanism of initial borazine formation is unclear and involvement of trace amounts of impurities cannot be ruled out.

#### *B,B',B''*-Trichloro-*N,N',N''*-tri(*p*-fluorophenyl)borazine (**3a**)

As reported in the literature, borazines **3** can usually be obtained by heating the 1:1-adduct **1** in refluxing benzene or toluene.<sup>40,50</sup> The same is true for the 1:1 adduct **1a** that forms between *p*-fluoroaniline and boron trichloride. After heating to  $100^\circ\text{C}$  for 19 hours in toluene, the  $^{11}\text{B}$  NMR signal of the tetra-coordinated boron atom has disappeared and a new signal at  $\sim 32$  ppm is observed. This is within the range typical of trichloroborazines. The compound can be isolated by evaporation of the solvent. The EI-MS spectrum gives the  $\text{M}^+$  peak  $(\text{ArNBCl})_3$  along with peaks due to fragmentation of the borazine core to the diazadiboretidine  $(\text{ArNBCl})_2$  and iminoborane  $\text{ArNBCl}$ .

Crystals of the borazine **3a**, prepared in refluxing toluene as described above, were obtained by slow evaporation of toluene from a concentrated solution. Compound **3a** crystallizes in the monoclinic system, space group  $P21/c$  and  $Z = 4$  (Fig. 3).

#### NMR reaction monitoring

The transformation of **1a** into **3a** was followed by  $^{19}\text{F}$  and  $^{11}\text{B}$  NMR spectroscopy. In order to collect the reaction data, to a solution of boron trichloride (1 M in hexanes, 1.24 eq.) in toluene

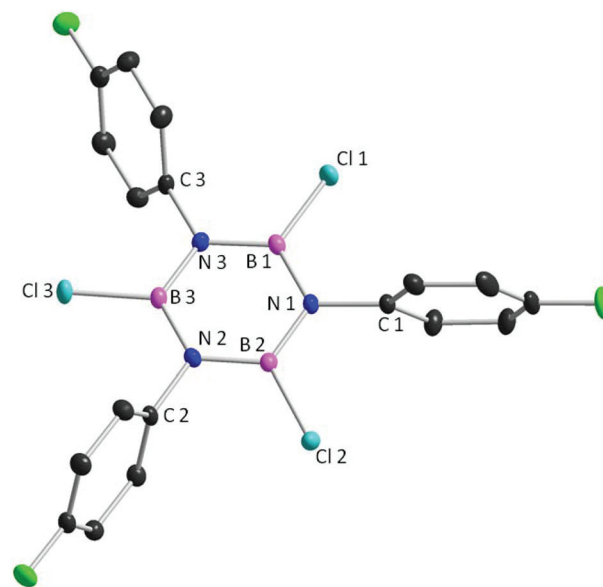


**Fig. 3** The molecular structure of **3a** in the crystal prepared in refluxing toluene; selected bond lengths (in Å) and bond angles (in  $^\circ$ ): N1–B1 1.436(3), N1–B3 1.436(3), N2–B1 1.431(3), N2–B2 1.435(3), N3–B2 1.432(3), N3–B3 1.421(3), B1–Cl1 1.762(2), B2–Cl3 1.764(3), B3–Cl2 1.770(2), N1–C1 1.450(3), N2–C7 1.449(3), N3–C13 1.453(3); C1–N1–B1 120.3(2), C1–N1–B3 120.0(2), B1–N1–B3 119.7(2), C7–N2–B1 120.2(2), C7–N2–B2 119.9(2), B1–N2–B2 119.8(2), C13–N3–B2 119.6(2), C13–N3–B3 120.0(2), B2–N3–B3 120.3(2), N1–B1–N2 120.0(2), N1–B1–Cl1 120.1(2), N2–B1–Cl1 119.9(2), N2–B2–N3 119.8(2), N2–B2–Cl3 119.9(2), N3–B2–Cl3 120.2(2), N1–B3–N3 120.1(2), N1–B3–Cl2 119.6(2), N3–B3–Cl2 120.4(2). Hydrogen atoms omitted for clarity.

was added a solution of 4-fluoroaniline in toluene (1.00 eq.) at  $0^\circ\text{C}$ , which resulted in the immediate precipitation of **1a**. Then the mixture was heated under a constant argon flow and NMR samples were collected from the reaction vessel after complete dissolution. The samples were immediately diluted with deuterated solvent and measured at room temperature. Under these conditions, homogeneous solutions were obtained. The  $^{19}\text{F}$  NMR spectrum only displayed three major peaks at  $-112.0$  ppm,  $-117.2$  ppm, and  $-115.5$  ppm. The carriers of the signals at  $-112.0$  ppm and  $-115.6$  ppm can be assigned to the 1:1 adduct **1a** ( $-112.0$  ppm) and borazine **3a** ( $-115.6$  ppm), respectively, based on the  $^{19}\text{F}$  NMR shifts of separately obtained samples (see above). During the course of the reaction the intensity of the signal at  $-112.0$  ppm (*i.e.*, the 1:1 adduct **1a**) decays and that of  $-117.2$  ppm (anilindichloroborane **2a**, see below for assignment) goes through a maximum (Fig. 4). After a standard reaction time<sup>29,37,40</sup> of 19 h the data of the  $-115.6$  ppm signal (*i.e.*, borazine **3a**) pointed to a limit. As already mentioned in the literature,<sup>39</sup> *B,B',B''*-trichloroborazines are unstable upon prolonged heating and **3a** likewise decomposed after 3 d at  $100^\circ\text{C}$  as seen by the disappearance of the peak at  $-115.6$  ppm in the fluorine NMR and the formation of an insoluble material.

Data acquisition at the beginning of the reaction is problematic: the zero-point of the kinetic measurements is difficult

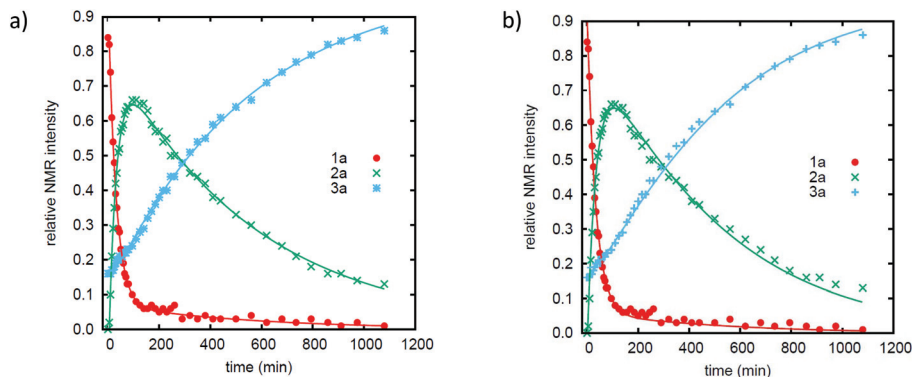


Fig. 4 Data points obtained by  $^{19}\text{F}\{^1\text{H}\}$  NMR in relative intensities using the signals at  $-112.0$  ppm (**1a**, red),  $-117.2$  ppm (**2a**, green) and  $-115.6$  (**3a**, blue). (a) Fit of the experimental data to the reaction mechanism shown in Scheme 3; (b) fit of the experimental data to the reaction mechanism of Scheme 4.

to determine as stable signals can only be obtained after the complete dissolution of the initially formed precipitate. Also, the short sample collection interval did not allow direct transfer to the NMR spectrometer, so the first 15 samples were stored at  $0^\circ\text{C}$  and were measured approximately one hour later. The measured samples were homogeneous solutions. The effect of prolonged standing in an ice bath should not have a dramatic effect on the shape of the NMR spectrum as **1a** is stable under these conditions and the temperature difference of  $\Delta T = 100$  K is expected to lead to a drastic slowdown of the reaction of **2a**. Nevertheless, the trace of **3a** shows an offset of about 0.15 units that we attribute to a parallel reaction that quickly forms borazine **3a** at  $0^\circ\text{C}$  (see above). Note that Mooney and Gerrard<sup>39</sup> could also detect  $B, B', B''$ -trichloroborazines at  $-80^\circ\text{C}$  together with dichloroaminoborane in the dichloromethane phase in the reaction mixture of aniline and boron trichloride.

Besides  $^{19}\text{F}\{^1\text{H}\}$  NMR investigations,  $^{11}\text{B}\{^1\text{H}\}$  NMR spectra were acquired. To suppress background signals, measurements were run in quartz NMR tubes. The boron spectra showed two peaks at 6.5 and 32.0 ppm, but deconvolution of the latter peak revealed two signal subsets with different halfwidths (70 Hz and  $>200$  Hz). Due to the overlap of the  $^{11}\text{B}$  NMR signals, only a few important data points were measured (ESI, Fig. S2†). The intensities of these three peaks line up perfectly with the data obtained from  $^{19}\text{F}$  NMR. Due to the uncertainties of the deconvolution, the  $^{11}\text{B}$  data were not employed for kinetic analysis.

Note that the  $^{19}\text{F}$  NMR spectra did not display the peak of free 4-fluoroaniline. The small excess of boron trichloride (0.24 eq.) was detectable by  $^{11}\text{B}$  NMR only during the first 60 min before it was presumably taken away by the argon stream. Running the experiment in sealed NMR tubes proved to be disadvantageous because the formation of **3a** was very strongly slowed down and a multitude of novel and unassigned  $^{19}\text{F}$  NMR signals appeared. This demonstrates the importance of removal of volatile products (like HCl) from the reaction mixture, which was achieved by employing a controlled stream of argon (see Experimental details).

### Assignment and properties of the intermediate of borazine formation

The NMR investigations confirmed the involvement of an intermediate that can be assigned to anilino-boron dichloride **2a**, as explained in this section. Isolation of the intermediate **2a** was not successful. Stopping the reaction at the highest concentration of **2a** and evaporating the solvent at room temperature under vacuum resulted in compounds **1a** and **3a**. Attempts to crystallize **2a** at this stage of the reaction led again to the same disproportionation. Similar observations were made by Bartlett *et al.*,<sup>38</sup> who identified the 1 : 1 adduct and borazine instead of the expected anilino-boron dichloride ( $\text{ArNHBCl}_2$ ) when they stopped the reaction after the elimination of *ca.* one mole of hydrogen chloride per mole of 1 : 1 adduct. To further characterize **2a**, the  $^{15}\text{N}\text{-}^1\text{H}$ -HSQC-DEPT NMR spectrum was measured immediately after stopping the reaction at the highest concentration of **2a**. This NMR experiment gives cross-peaks for hydrogen atoms bound to nitrogen, and indeed two such signals can be found. One is due to **1a** ( $^{15}\text{N}$  77.8 ppm;  $^1\text{H}$  4.8 ppm) by comparison with the known  $^1\text{H}$  NMR shift of the isolated material, and another one is assigned to **2a** ( $^{15}\text{N}$  117.0 ppm;  $^1\text{H}$  5.4 ppm). In addition, the DEPT experiment shows that the phases of the two peaks are opposite. As **1a** has two protons bound to nitrogen; the opposite phase for **2a** suggests that only one or three protons are bound to its nitrogen atom. As three protons and the aryl group would result in an anilinium ion, the only reasonable conclusion is that **2a** has one proton bound to nitrogen. Taking into account the  $^{11}\text{B}$  NMR shift of 32 ppm as an additional constraint, only leaves the monomeric aminodichloroborane ( $\text{ArNHBCl}_2$ ) **2a** as a reasonable proposal for the intermediate. Its cyclodimer or cyclotrimer is expected to show  $^{11}\text{B}$  NMR chemical shifts in the range of tetracoordinated boron atoms and hence can be excluded as possible carriers of the signals associated with the intermediate. The assignment to **2a** is further supported by computations of the chemical shifts at the KT3/pcS-3//SCS-MP2/cc-pVTZ level of theory (see Computational methods for details). These arrive at values of

−114.9 ppm for  $^{19}\text{F}$  (exp. −117 ppm), 30.4 ppm for  $^{11}\text{B}$  (exp. 32 ppm), and 119.7 ppm for  $^{15}\text{N}$  (exp. 117 ppm).

We also probed the stability of **2a** with respect to reaction with free boron trichloride and 4-fluoroaniline by stopping the reaction close to the maximum concentration of **2a** (obtained from an equimolar amount of reagents) and adding either of the reagents at room temperature. While **2a** does not react with boron trichloride to an appreciable amount, it reacts instantaneously with 4-fluoroaniline to give  $(\text{ArNH})_2\text{BCl}$  **5a** as the major product according to NMR. This experiment suggests that the lifetime of **2a** could be limited by the absence or presence of free 4-fluoroaniline.

### Computational investigations

To shed light on the barriers for HCl elimination from **1a** and **2a**, computational investigations were performed at the CCSD(T)/cc-pVTZ//SCS-MP2/cc-pVTZ level of theory (for details see Computational methods). As the reaction was run in the non-polar toluene, the influence of solvent was neglected in the computations. The boron–nitrogen bond in the 1 : 1 adduct **1a** has a bond dissociation energy  $D_0$  of 22.3 kcal mol $^{-1}$  for the formation of *p*-fluoroaniline and boron trichloride. Taking into account entropy and thermal corrections using the rigid rotor harmonic oscillator model shows that the dissociation of the 1 : 1 adduct **1a** is endoergic at the temperature of the experiment ( $\Delta_{373.15}G = +7.7$  kcal mol $^{-1}$ ). We could identify a transition state for the unimolecular elimination of hydrogen chloride from the 1 : 1 adduct **1a**. Its structure (ESI, Fig. S28†) is very similar to that identified for hydrogen chloride elimination from  $\text{BCl}_3\text{NH}_3$  earlier.<sup>44,45</sup> It is most remarkable that one boron–chlorine bond is essentially already broken (distance: 2.68 Å), while the chlorine–hydrogen distance is still rather long (1.67 Å), indicative of a late transition state. The hydrogen chloride elimination is mildly exergonic ( $\Delta G_{373.15}^0 = -3.8$  kcal mol $^{-1}$ ) with  $\Delta G_{373.15}^\ddagger = 27.6$  kcal mol $^{-1}$ . Using the Eyring equation, this free energy of activation corresponds to  $k = 3.18 \times 10^{-2}$  min $^{-1}$ . This is in very good agreement with the rate constant  $k_1 = 3.03(7) \times 10^{-2}$  min $^{-1}$  derived from fitting the kinetic data (see below).

The computations show that the elimination of another molecule of hydrogen chloride from the anilindichloroborane **2a** to give the iminoborane  $\text{ArN}(\text{BCl})_2$  has a much higher free energy of activation,  $\Delta G_{373.15}^\ddagger = 67.9$  kcal mol $^{-1}$ . For this reason, the formation of the iminoborane (followed by its rapid cyclotrimerization to **3a**) is not feasible under experimental conditions. Due to a similarly high barrier for unimolecular hydrogen chloride elimination from the parent aminodichloroborane ( $\text{BCl}_2\text{NH}_2 \rightarrow \text{BClNH} + \text{HCl}$ ) this reaction was judged to be unimportant by Allendorf and Melius<sup>44</sup> for the

formation of boron nitride from ammonia and boron trichloride under CVD conditions. Indeed, iminoborane could not be detected by mass spectrometry in a flow reactor under CVD conditions.<sup>43</sup>

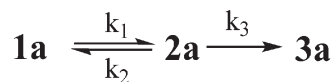
We also computed barriers for the reaction of anilindichloroborane **2a** with free 4-fluoroaniline or boron trichloride and subsequent loss of HCl, as these reactions were probed experimentally, but only that with 4-fluoroaniline was observed. Due to system size, the geometry of the compounds was optimized with the more economic M06-2X/6-311+G\*\* method (for details see Computational methods) while energies were refined using CCSD(T)/cc-pVTZ single energy point computations. Anilinoborane **2a** forms an adduct with 4-fluoroaniline in a mildly endergonic reaction ( $\Delta_{373.15}G = +5.7$  kcal mol $^{-1}$ ) to give **2aA** (Scheme 2, see ESI, Fig. S29† for computed structures), while the formation of the adduct **2aB** with boron trichloride is strongly endergonic ( $\Delta G_{373.15}^0 = +15.7$  kcal mol $^{-1}$ ). Elimination of HCl from **2aA** to **5a** can proceed with a barrier  $\Delta G_{373.15}^\ddagger = 17.9$  kcal mol $^{-1}$  while that of **2aB** to **6a** has a higher barrier  $\Delta G_{373.15}^\ddagger = 24.7$  kcal mol $^{-1}$ .

Based on reactants **2a** and aniline or boron trichloride, the formation of  $(\text{ArNH})_2\text{BCl}$  is much more favorable than that of  $\text{ArN}(\text{BCl}_2)_2$ , in agreement with the experimental observations. These calculations show that the reactive intermediate **2a** can readily react with free aniline under experimental conditions.

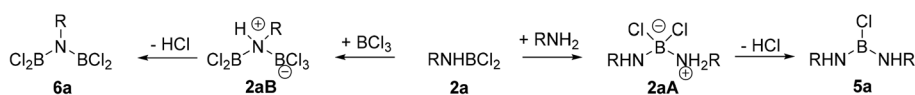
### Kinetic data fitting

The traces of the compounds **1a**, **2a**, and **3a** were fitted with the kinetic schemes displayed in Scheme 3 and Scheme 4. The rate constants were determined in a least-squares fit between the experimental traces and calculated values obtained by numerically solving the set of first order initial value differential equations with the fourth-order Runge-Kutta method.<sup>55</sup> The fit was performed using the Marquardt method and incorporated variational optimization of the initial concentrations.

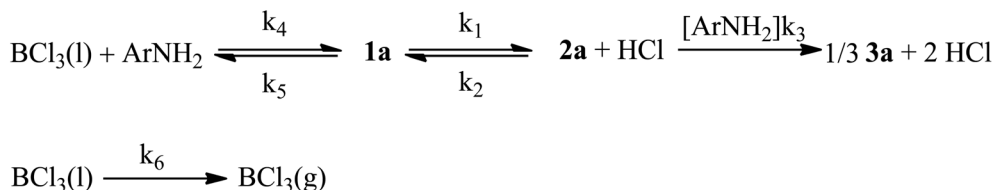
The lines in Fig. 4a represent the fitted result of this procedure for Scheme 3 which provide first order rate constants  $k_1 = 3.03(7) \times 10^{-2}$  min $^{-1}$ ,  $k_2 = 2.5(3) \times 10^{-3}$  min $^{-1}$ , and  $k_3 = 1.97(3) \times 10^{-3}$  min $^{-1}$ . It was attempted to perform the fit with various alternative fitting schemes such as avoiding the back reaction from **2a** to **1a** or including a second order reaction in **2a** from **2a** to **3a** and second order reactions of **2a** with the boron trichloride or aniline concentrations. However, these



Scheme 3 Kinetic scheme used to fit the observed traces in Fig. 4a.



Scheme 2 Reaction of **2a** with 4-fluoroaniline and boron trichloride.



**Scheme 4** Alternative kinetic scheme involving dissociation of **1a** used to fit the traces in Fig. 4b.

fits provided a significantly poorer representation of the measured values.

As Scheme 3 is not consistent with the very high barrier computed for the unimolecular HCl elimination from **2a** (to give iminoborane ArN=BCl, see the section Computational investigations), we also considered the alternative kinetic scheme that involves the reaction of free 4-fluoroaniline with **2a** (Scheme 4).

Here, **1a** is in equilibrium with **2a** and HCl *via* first order reactions in these compounds. Hereby we assume a constant (steady state) concentration of HCl, which is formed in the reaction and simultaneously evaporates from the reaction mixture. Furthermore, **1a** is in equilibrium with its dissociation products, the trichloroborane in the liquid phase, BCl<sub>3</sub>(l), and the aniline, RNH<sub>2</sub>. The latter reacts in a second order reaction with **2a** to give an adduct (**2aA**, Scheme 2) that leads, in several steps, to borazine **3a**. In that reaction, two further molecules of **2a** are consumed and three molecules of HCl and one molecule of RNH<sub>2</sub> are produced. In an additional step, BCl<sub>3</sub>(l) evaporates from the solution to the gas phase molecule, BCl<sub>3</sub>(g), with a rate constant *k*<sub>6</sub>. The latter is likely to happen under the reaction conditions due to the low boiling point of BCl<sub>3</sub> (12.5 °C) and the argon flow conditions. Rate constants and initial concentrations were optimized to reproduce the measured concentrations. However, the NMR spectra were measured at room temperature where boron trichloride and fluoroaniline react with **1a**, which was assumed in the simulation of the observed concentrations. A fit of the rate constants provided the concentration profiles shown in Fig. 4b.

As shown in Fig. 4b, Scheme 4 allows for an appropriate reproduction of the evolution of the observed concentrations. Thus, a kinetic scheme involving the reaction of **2a** with aniline discussed above as a key step is a realistic alternative to the pleasantly simple Scheme 3.

## Discussion

### Previous mechanistic suggestions

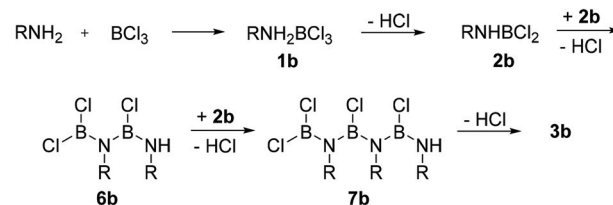
In the literature, three mechanistic suggestions were made that will be briefly sketched below. A first-order hydrogen chloride evolution obtained for the last phase (roughly the last 10% due to poor solubility of the 1 : 1 adduct in benzene) of the reaction led Gerrard and Mooney<sup>39</sup> to the assumption that aniline, *p*-toluidine, and *p*-bromoaniline first form an adduct **1**

with boron trichloride that undergoes successive hydrogen chloride evolution and proceeds *via* the aminodichloroborane **2** (Scheme 1).<sup>39</sup>

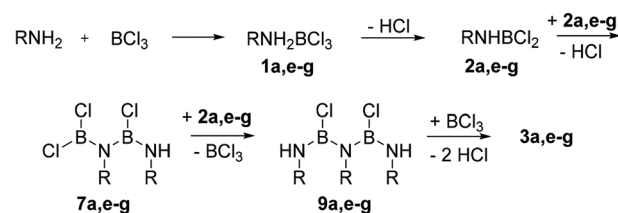
Bartlett *et al.* observed that the thermal evolution of hydrogen chloride from the aniline–trichloroborane adduct is initially first order and turns to second order in the course of the reaction.<sup>38</sup> Hence, these authors specifically ruled out Gerrard and Mooney's mechanistic proposal. Their suggestion (Scheme 5) is bimolecular formation of the four- and six-membered chains **7** and **8**, respectively, by connecting three aminoborane molecules **2**. The last step transforms the open chain array into the borazine ring system **3** by a unimolecular ring closure.<sup>38</sup>

Atkinson *et al.*<sup>40</sup> likewise assumed the intermediacy of short chains like **7** and **9** formed in bimolecular reactions with hydrogen chloride and boron trichloride elimination (Scheme 6). The produced boron trichloride closes the chain to the borazine ring **3**.

This proposal rests on the finding that monomeric aminodichloroboranes are known to form from the reaction of boron trichloride with aromatic amines with *o,o'*-disubstitution, and in this case these can be isolated.<sup>40,49,50,56</sup> However, such *o,o'*-disubstituted anilindichloroboranes cannot be transformed thermally into borazines. Further thermal hydrogen chloride



**Scheme 5** Mechanism proposed by Bartlett *et al.*<sup>38</sup> (b: R = Ph).



**Scheme 6** Mechanism proposed by Atkinson *et al.*<sup>40</sup> (a: R = *p*Ph, e: R = *m*ClPh, f: R = *o*BrPh, g: R = *m*BrPh).

elimination produces chains,<sup>38,40</sup> but such chains do not cyclize to borazines with the added boron trichloride.<sup>40</sup> However, *o,o'*-disubstituted anilindichloroboranes form borazines upon reaction with triethylamine.<sup>38</sup>

It should also be noted that there may exist mechanistic alternatives depending on the acidity of the aniline and steric demand of substituents. For example, *ortho*-toluidine (*o*-CH<sub>3</sub>C<sub>6</sub>H<sub>4</sub>NH<sub>2</sub>) was found to undergo hydrogen chloride elimination by two consecutive first-order reactions with quite different rates.<sup>30</sup> After loss of one mole of hydrogen chloride, the aminoborane intermediate can be isolated.<sup>30</sup> Furthermore, adducts of aliphatic primary amines and boron trichloride evolve hydrogen chloride in fractional-order reactions and initial equilibrium and a chain reaction were suggested for explanation.<sup>30</sup>

### Discussion of the mechanism

Taking all information and arguments together, we suggest a reaction sequence for the formation of borazine **3a** from 4-fluoroaniline and boron trichloride that starts with the formation of a poorly soluble 1 : 1 Lewis acid–base adduct **1a** at 0 °C, which fully dissolves at 100 °C and undergoes unimolecular hydrogen chloride elimination to give the anilindichloroborane **2a**. This first step is reversible.

For the reaction anilindichloroborane (**2a**) →  $\frac{1}{3}$  borazine (**3a**) + HCl no additional intermediates could be identified in the NMR study. The fact that the conversion of intermediate **2a** is first order in **2a** allows discarding mechanisms that require the bimolecular reaction of **2a** to give chains or the cyclodimer and cyclotrimer of **2a** as rate limiting steps. The most obvious mechanistic alternative would be the transformation of **2a** into chloroiminoborane RNBCl and hydrogen chloride. However, the computations show that this pathway is associated with a prohibitively high energy barrier. We therefore discard this mechanism even though it is simple and compatible with the measured kinetics (see Fig. 3a). Note that the involvement of iminoboranes was implied in early work on borazine formation and borazine decomposition by dry hydrogen chloride reported by Wiberg and co-workers, but the corresponding reactions were run at much higher temperatures than those studied here.<sup>57–60</sup> Avent *et al.* suggested the involvement of the iminoborane BCINH in the closely related reaction of ammonia and boron trichloride that produces trichloroborazine (BCINH)<sub>3</sub>, but conceded that the evidence for intermediates other than the 1 : 1 adduct, which they could characterize by X-ray structural analysis and NMR spectroscopy in solution, is circumstantial.<sup>47</sup> Indeed, the gas phase study of the reaction of boron trichloride and ammonia concluded that the corresponding iminoborane is not involved (see above).<sup>43</sup>

The first order disappearance of anilindichloroborane **2a** is difficult to reconcile with a plausible mechanism, unless it is pseudo first order due to a stationary concentration of some intermediate. This suggestion is in agreement with Blackborow *et al.*,<sup>50</sup> who observed previously that 2-bromoanilindichloroborane did not undergo borazine formation once isolated from the reaction mixture and heated in a pure form

in solution. These authors thus concluded that catalysis is required for the transformation of **2** into **3**, a conjecture that also seems likely for the system studied here.

An important observation in our study is the finding that **2a** reacts rapidly with free 4-fluoroaniline to afford the dianilinochloroborane [(C<sub>6</sub>H<sub>4</sub>FNH)<sub>2</sub>BCl] **5a**, and the computational confirmation of a low-energy pathway. 4-Fluoroaniline could arise along with boron trichloride from the dissociation of the adduct **1a** in hot toluene. According to our CCSD(T)/cc-pVTZ//SCS-MP2/cc-pVTZ computations this process is endergonic by +7.7 kcal mol<sup>-1</sup>, which would result in a low concentration of the free 4-fluoroaniline and BCl<sub>3</sub> (log *K*<sub>373</sub> = -4.5). The volatile BCl<sub>3</sub> would be removed along with the HCl reaction product in the argon stream. We would not have been able to detect free 4-fluoroaniline by NMR spectroscopy, as this was done at room temperature where the equilibrium is very far on the side of the adduct **1a**.

The reaction mechanism of Scheme 4 is based on these arguments and indeed is able to provide an acceptable fit of the experimental data. We therefore suggest that the availability of 4-fluoroaniline to react with the transient reactive intermediate **2a** to afford **5a** and HCl limits the rate of the reaction to borazine. The importance of free 4-fluoroaniline for the course of the reaction can also explain why a small fraction of borazine **3a** is already formed during the addition of reagents before heating. In this scenario, formation of the Lewis acid–base adduct **1a** is a dead end, and heating is required for the production of reactive compounds with HCl elimination being the first step.

As is always the case with kinetic analyses, statements on reactions after the rate-determining step are speculative. Hence, it is not clear how **5a** transforms into **3a**, but a comparison with amine-borane adducts, RNH<sub>2</sub>BH<sub>3</sub>, may be instructive. There, the involvement of cyclotriborazanes, (RNHBH<sub>2</sub>)<sub>3</sub>, has been established in catalyzed dehydrogenation reactions leading to borazines (RNBH)<sub>3</sub>.<sup>61,62</sup> In the case of aromatic amines, Helten *et al.*<sup>63</sup> concluded that borazines “are not simply formed by dehydrogenation of cyclotriborazanes”. Rather, dianilinoborane (PhNH)<sub>2</sub>BH was found to transform the cyclotriborazane into the borazine with concomitant regeneration of the aniline–borane adduct.<sup>63</sup> Thermal dehydrochlorinations are generally more facile than dehydrogenations, and accordingly, fewer intermediates were observed in our study. While the intermediacy of chains or cycles, such as the chloro-derivatives of cyclotriborazane, cannot be excluded, the kinetics are not in agreement with their formation as rate limiting steps.

## Conclusions

The present investigation used NMR spectroscopy (<sup>19</sup>F and <sup>11</sup>B) to investigate the mechanism of borazine formation from 4-fluoroaniline (ArNH<sub>2</sub>) and boron trichloride in toluene at 100 °C. The study shows that the initially formed 1 : 1 adduct (**1a**) transforms into borazine **3a** involving ArNHBCl<sub>2</sub> (**2a**) as

the only detectable reactive intermediate. The assignment to **2a** is based on NMR spectral data and is supported by computed chemical shifts using density functional theory. The hydrogen chloride elimination from **1a** is a first order reaction in **1a**. The computed activation free energy (CCSD(T)/cc-pVTZ//SCS-MP2/cc-pVTZ) is in good agreement with the measured rate constant for the hydrogen chloride elimination (**1a** → **2a** + HCl). As no intermediates were observed for the transformation **2a** → 1/3 **3a** + HCl, definite conclusions are difficult to draw. The formation of the iminoborane (RNBCl) from **2a** by hydrogen chloride elimination is excluded based on the very high barriers associated with this step. More likely are processes involving free aniline and boron trichloride, which may be produced in low concentrations from the 1:1 adduct **1a**. The observed facile reaction of **2a** with 4-fluoroaniline to afford di-(4-fluorophenyl)aminoborane **2aA** suggests that this is a key reaction in the mechanism, which is compatible with the measured concentration profiles.

## Experimental details

### General

All reactions were carried out under an inert atmosphere using argon as a protective gas. Dry toluene was obtained from a solvent purification system (MBraun SPS-800). Boron trichloride (1 M in hexanes) was purchased from Acros, 4-fluoroaniline was obtained from ABCR and distilled (25 mbar, 74 °C) prior to use. All NMR spectra were recorded on Bruker DRX 250, Avance II 400, Avance II+, Avance III HD 400, and Avance III HDX 600 spectrometers. The NMR spectra were measured at room temperature in C<sub>6</sub>D<sub>6</sub> (dried over molecular sieves 4 Å) that was purchased from Deutero GmbH. The spectra were referenced either to residual solvent signals (<sup>1</sup>H, <sup>13</sup>C: SiMe<sub>4</sub>)<sup>64</sup> or externally (<sup>19</sup>F: CCl<sub>3</sub>F, <sup>11</sup>B: BF<sub>3</sub>·OEt<sub>2</sub>). <sup>11</sup>B solid-state NMR spectra were measured with a Bruker DSX-200 instrument at 64 MHz in a 4 mm ZrO<sub>2</sub> rotor referenced to NaBH<sub>4</sub> and δ<sub>iso</sub>, χ, and η were determined using the program WSpin. The deconvolution of the <sup>11</sup>B spectra was done with TopSpin.<sup>66</sup> DRIFTS measurements were performed with a NICOLET 6700 FTIR spectrometer (Thermo Scientific) and dried KBr powder was used as a dilution matrix (10 wt% analyte related to m<sub>analyte</sub> + m<sub>KBr</sub> = 100%). The sample-KBr mixture was always intimately mixed by grinding in an agate mortar prior to the measurements and put into a DRIFTS cell with KBr windows. The collected data were converted using the Kubelka-Munk refinement. For EI-MS measurements a MSD 5977 Agilent MSD and for HR-EI-MS measurements a MAT95 Finnigan spectrometer was used. Elemental analysis was done with a varioMICROcube (Elementar Analysensysteme GmbH (Hanau)) in the CHNS modus.

### Synthesis

**Compound 1a.** At 0 °C, a solution of 21 mL (21 mmol) boron trichloride (1 M in hexanes) in 40 mL of toluene (abs.) was charged with a solution of 1631 μL (17 mmol) 4-fluoro-

aniline in 10 mL of toluene (abs.) within 5 min, immediately leading to a colorless precipitate. Then the dropping funnel was washed with 5 mL of toluene (abs.) and the cold suspension was filtered through a frit. The remaining solid was dried under vacuum (1.7 g; 35.5%).

EA for C<sub>6</sub>H<sub>6</sub>BCl<sub>3</sub>FN: calc. C 31.57%, N 6.14%, H 2.65%, found C 31.51%, N 6.30%, H 2.57%; DRIFT-IR (KBr, cm<sup>-1</sup>): 3190 s, 3174 s, 3090 m, 2599 w, 2530 w, 2525 w, 2495 w, 2398 w, 1888 w, 1604 w, 1562 m, 1511 s, 1444 w, 1308 s, 1240 m, 1230 m, 1199 m, 1161 m, 1100 m, 1014 w, 939 w, 908 s, 893 s, 851 s, 831 m, 800 m, 792 m, 774 s, 717 m, 700 m, 686 m, 667 m, 630 w, 547 s, 492 m, 429 w; <sup>1</sup>H (400 MHz, C<sub>6</sub>D<sub>6</sub>): 4.84 (s, 2H, NH<sub>2</sub>), 6.47 (s, 2 H, Ar), 6.46 (s, 2 H, Ar); <sup>19</sup>F{<sup>1</sup>H} (376 MHz, C<sub>6</sub>D<sub>6</sub>): -112.0; <sup>11</sup>B{<sup>1</sup>H} (80 MHz, C<sub>6</sub>D<sub>6</sub>): 6.5; <sup>11</sup>B (64 MHz, MAS, R<sub>f</sub> 10 kHz): δ<sub>iso</sub> 6.1.

**Compound 3a.** A solution of 1 g (4.4 mmol) **1a** in 20 mL toluene (abs.) was heated to 100 °C with a gentle argon flow passing over the mixture. After 19 h the solvent was evaporated under vacuum at room temperature. Slightly yellow microcrystals were obtained with impurities due to partial decomposition of **3a** (475 mg; 23%).

<sup>1</sup>H (400 MHz, C<sub>6</sub>D<sub>6</sub>): 6.7–6.8 (m, 4H, Ar); <sup>19</sup>F{<sup>1</sup>H} (376 MHz, C<sub>6</sub>D<sub>6</sub>): -115.5; <sup>11</sup>B{<sup>1</sup>H} (80 MHz, C<sub>6</sub>D<sub>6</sub>): 32.0 (>200 Hz); EI-MS (*m/z*): 465 [M<sup>+</sup>, (FARNBCl)<sub>3</sub>], 310 [M<sup>+</sup>, (FARNBCl)<sub>2</sub>], 155 [M<sup>+</sup>, (FARNBCl)]; HR-EI-MS for C<sub>18</sub>H<sub>12</sub>B<sub>3</sub>Cl<sub>3</sub>F<sub>3</sub>N<sub>3</sub>: calc. 465.032808, found 465.03587.

**Compound 4a.** To a solution of trisdimethylaminoborane (0.5 mL, 2.86 mmol) in toluene (22 mL) was added 4-fluoroaniline (0.81 mL, 8.58 mmol). The mixture was refluxed for 36 hours and turned from yellow to red-brown during this time. During slow cooling to room temperature, crystals formed overnight, which were isolated (0.41 g, 61%).

<sup>1</sup>H (400 MHz, C<sub>6</sub>D<sub>6</sub>): 6.72 (m, 6 H), 6.47 (m, 6 H), 4.14 (br s, 3 H); <sup>13</sup>C (100 MHz, C<sub>6</sub>D<sub>6</sub>): 116.1 (d, *J* = 22.32 Hz), 121.8 (d, *J* = 7.44 Hz), 139.9 (d, *J* = 2.67 Hz), 158.3 (d, *J* = 239.50 Hz); <sup>19</sup>F{<sup>1</sup>H} (376 MHz, C<sub>6</sub>D<sub>6</sub>): -122.7; <sup>11</sup>B{<sup>1</sup>H} (80 MHz, C<sub>6</sub>D<sub>6</sub>): 23.5; <sup>11</sup>B (64 MHz, MAS, R<sub>f</sub> 10 kHz): δ<sub>iso</sub> 23.5 ppm, χ = 2.40 Hz, η = 0.17; EI-MS (*m/z*): 341 [M<sup>+</sup>], 230 [FARNBNHArF<sup>+</sup>], 111 [FARNH<sub>2</sub><sup>+</sup>]; HR-EI-MS: calc. 341.13056 Da, found 341.13210 Da.

**Compound 5a.** To a solution of 12 mg (0.05 mmol) **1a** in benzene (2.5 mL) were added 12 μL (0.11 mmol) 4-fluoroaniline. The immediate formation of a very fine colorless suspension was observed. The NMR spectral data of this suspension given below are in agreement with essentially quantitative formation of **5a**. Attempts to isolate **5a** by removal of the solvent under vacuum always resulted in mixtures of **5a** and **4a** that could not be separated.

<sup>1</sup>H (400 MHz, C<sub>6</sub>D<sub>6</sub>): 4.60 (br s, 2 H), 6.49–6.52 (m, 4 H), 6.64–6.70 (m, 4 H); <sup>13</sup>C (100 MHz, C<sub>6</sub>D<sub>6</sub>): 115.9 (d, *J* = 22.52 Hz), 124.1 (d, *J* = 7.73 Hz), 137.7 (d, *J* = 2.85 Hz), 159.5 (d, *J* = 242.41 Hz); <sup>19</sup>F (376 MHz, C<sub>6</sub>D<sub>6</sub>): -120.1; <sup>11</sup>B (80 MHz, C<sub>6</sub>D<sub>6</sub>): 26.3.

### Kinetic measurements

To guarantee optimal argon flow, the reaction exhaust is passed only through CaCl<sub>2</sub> and a commonly used water or pot-

assium hydroxide washing flask is omitted. During the reaction monitoring, each collected sample (0.3 ml reaction mixture) was transferred *via* a syringe to a NMR tube filled in the glovebox with 0.2 ml C<sub>6</sub>D<sub>6</sub> and sealed with a septum before <sup>19</sup>F{<sup>1</sup>H} or <sup>11</sup>B{<sup>1</sup>H} spectra were measured. Although no information relevant for the reaction can be gathered from measuring hydrogen nuclei (due to the manifold excess of the nondeuterated toluene solvent) <sup>1</sup>H NMR spectra were acquired for every sample to check the field homogeneity.

**Kinetic experiment 1.** At 0 °C, to a solution of 21 mL (21 mmol) boron trichloride (1 M in hexanes) in 40 mL of toluene (abs.) was added a solution of 1631 µl (17 mmol) 4-fluoroaniline in 10 mL of toluene (abs.) within 5 min, immediately leading to a colorless precipitate. Then the dropping funnel was washed with 5 ml of toluene (abs.) and the argon inlet was switched so that argon is passing gently over the mixture. The suspension was stirred for another 20 min at 0 °C and then heated to 100 °C within 20 min while the precipitate dissolved after 10 min. The first sample was collected when the reaction reached 100 °C and the following samples at intervals of 30 min (up to 3.5 h, samples 1–8). Sample 9 was taken after 4.5 h, sample 10 after 19 h and samples 11, 12 and 13 after 43.5, 68.5 and 116.5 h, respectively. <sup>11</sup>B{<sup>1</sup>H} NMR measurements were performed on samples 1–6 and 10, 11, and 13. The boron and fluorine NMR spectra of samples 11–13 showed increasing amounts of decomposition products while the product peak (–115.5 ppm, 32.0 ppm) steadily vanished. After 116.5 h, the decomposition products were almost insoluble and precipitated from solution. The graph received from the fluorine NMR spectra of experiment 1 can be found in the ESI (Fig. S2†).

**Kinetic experiment 2.** At 0 °C, to a solution of 21 mL (21 mmol) boron trichloride (1 M in hexanes) in 40 ml of toluene (abs.) was added a solution of 1631 µl (17 mmol) 4-fluoroaniline in 10 ml of toluene (abs.) within 7.5 min, immediately leading to a colorless precipitate. Then the dropping funnel was washed with 10 ml of toluene (abs.) and the argon flow was set at 21 sccm min<sup>–1</sup>. The first sample was collected and the suspension was stirred for 15 min at 0 °C. After that, the reaction vessel was heated to 100 °C within 20 minutes while the precipitate dissolved at around 70 °C. The first 20 samples were collected with a 5 min (sample 20 at 107 min), samples 21–32 with a 15 min (sample 32 at 287 min), samples 33–38 with a 30 min (sample 38 at 467 min), and samples 39–47 with a 60 min interval. The last sample (48) was taken after 1107 min. The first three data points were obtained with samples that still contained some solid materials in the reaction mixture and were thus omitted from the kinetic analysis.

### X-ray crystallography

Crystals were grown by standard techniques from saturated solutions using toluene. Suitable single crystals for X-ray structure analyses were selected in a glovebox and coated with

Paratone-N (Hampton) and fixed on a nylon loop. Data for all crystals were collected using a Bruker APEX DUO instrument equipped with an IµS microfocus sealed tube and QUAZAR optics for MoK<sub>α</sub> radiation ( $\lambda = 0.71073 \text{ \AA}$ ). The data collection strategy for all was determined using COSMO<sup>67</sup> employing  $\omega$ - and  $\phi$  scans. Raw data were processed using APEX<sup>67</sup> and SAINT,<sup>67</sup> and corrections for absorption effects were applied using SADABS.<sup>68</sup> The structures were solved by direct methods and refined against all data by full-matrix least-squares methods on  $F^2$  using SHELXT<sup>69</sup> and Shelxle.<sup>70</sup> Further details of the refinement and crystallographic data are given in Table 1. CCDC numbers 1535682, 1535683, and 1590012† contain all the supplementary crystallographic data for this paper.

### Computational methods

Geometry optimizations were performed using spin-component scaled<sup>71,72</sup> Møller-Plesset second-order perturbation theory (SCS-MP2) in conjunction with the resolution-of-the-identity (RI)<sup>73</sup> and frozen-core approximations. Dunning's<sup>74</sup> correlation consistent triple- $\zeta$  basis set (cc-pVTZ) and the recommended<sup>75</sup> RI fitting basis set were employed. Due to the

**Table 1** Crystal data and structure refinements

	1a	3a	4a
Empirical formula	C <sub>6</sub> H <sub>6</sub> BCl <sub>3</sub> FN	C <sub>18</sub> H <sub>12</sub> B <sub>3</sub> Cl <sub>3</sub> F <sub>3</sub> N <sub>3</sub>	C <sub>18</sub> H <sub>15</sub> BF <sub>3</sub> N <sub>3</sub>
Formula weight	228.28	466.09	341.14
Temperature	100(2) K	100(2) K	100(2) K
Crystal system	Orthorhombic	Monoclinic	Triclinic
Space group	<i>Pca</i> 2 <sub>1</sub>	<i>P</i> 2 <sub>1</sub> / <i>c</i>	<i>P</i> $\bar{1}$
Unit cell dimensions	<i>a</i> = 11.2213(3) Å <i>b</i> = 12.4120(3) Å <i>c</i> = 6.7073(2) Å $\alpha = 90^\circ$ $\beta = 90^\circ$ $\gamma = 90^\circ$	<i>a</i> = 5.7426(2) Å <i>b</i> = 27.2822(10) Å <i>c</i> = 13.2120(5) Å $\alpha = 90^\circ$ $\beta = 101.990(2)^\circ$ $\gamma = 90^\circ$	<i>a</i> = 8.377(7) Å <i>b</i> = 10.109(9) Å <i>c</i> = 10.309(9) Å $\alpha = 99.27(2)^\circ$ $\beta = 112.227(16)^\circ$ $\gamma = 90.341(17)^\circ$
Volume	934.18(4) Å <sup>3</sup>	2024.78(13) Å <sup>3</sup>	795.5(12) Å <sup>3</sup>
<i>Z</i>	4	4	2
Density (calculated)	1.623 Mg m <sup>–3</sup>	1.529 Mg m <sup>–3</sup>	1.424 Mg m <sup>–3</sup>
Crystal size	0.193 × 0.075 × 0.045 mm <sup>3</sup>	0.313 × 0.080 × 0.064 mm <sup>3</sup>	0.268 × 0.133 × 0.080 mm <sup>3</sup>
Theta range for data collection	1.641 to 28.306°	1.576 to 29.596°	2.047 to 27.102°
Index ranges	–14 ≤ <i>h</i> ≤ 14 –16 ≤ <i>k</i> ≤ 16 –8 ≤ <i>l</i> ≤ 8	–7 ≤ <i>h</i> ≤ 7 –37 ≤ <i>k</i> ≤ 37 –18 ≤ <i>l</i> ≤ 18	–10 ≤ <i>h</i> ≤ 10 –12 ≤ <i>k</i> ≤ 12 –13 ≤ <i>l</i> ≤ 13
Reflections collected	10 743	38 758	24 544
Independent reflections	2231 [ <i>R</i> (int) = 0.0305]	5668 [ <i>R</i> (int) = 0.0407]	3483 [ <i>R</i> (int) = 0.0471]
Completeness to theta = 25.242°	99.9%	100.4%	99.7%
Goodness-of-fit on $F^2$	1.047	1.095	1.041
Final <i>R</i> indices [ <i>I</i> > 2σ( <i>I</i> )]	<i>R</i> <sub>1</sub> = 0.0258, <i>wR</i> <sub>2</sub> = 0.0629	<i>R</i> <sub>1</sub> = 0.0439, <i>wR</i> <sub>2</sub> = 0.1163	<i>R</i> <sub>1</sub> = 0.0402, <i>wR</i> <sub>2</sub> = 0.0977
<i>R</i> indices (all data)	<i>R</i> <sub>1</sub> = 0.0275, <i>wR</i> <sub>2</sub> = 0.0641	<i>R</i> <sub>1</sub> = 0.0521, <i>wR</i> <sub>2</sub> = 0.1258	<i>R</i> <sub>1</sub> = 0.0505, <i>wR</i> <sub>2</sub> = 0.1037

computational demand of the SCS-MP2 method, the geometries of larger systems (reactions  $\text{ArNHBCl}_2 + \text{BCl}_3$  and  $\text{ArNHBCl}_2 + \text{ArNH}_2$ ) were optimized using the M06-2X<sup>76</sup> hybrid density functional along with the 6-311+G\*\*<sup>77</sup> basis set employing the Gaussian 09 program.<sup>78</sup> The nature of stationary points as minima or transition structures was confirmed by computing second derivatives by finite differences of analytic gradients (SCS-MP2/cc-pVTZ)<sup>79</sup> or analytically (M06-2X/6-311+G\*\*). This produced harmonic vibrational frequencies that were employed without a scaling factor for computing enthalpy and entropy corrections using the approximation of an ideal gas and no coupling between degrees of freedom. The optimized geometries were employed in subsequent single point energy computations using coupled-cluster theory with singles, doubles, and a perturbative estimate of triple excitations, CCSD(T),<sup>80</sup> using the cc-pVTZ basis set.<sup>74</sup> The resolution of the identity (RI) approximation was used along with the corresponding fitting basis set.<sup>75</sup> All SCS-MP2 and CCSD(T) computations employed the frozen core approximation and were performed with the Turbomole program package.<sup>81</sup>

The Dalton program<sup>82,83</sup> was employed for the computation of the isotropic chemical shielding of **2a**, **4a**, and **5a** using the GIAO method and the KT3<sup>84</sup> functional along with the pcS-3<sup>85</sup> basis set. This choice of the functional and the basis set was motivated by the recommendations of Krivdin<sup>86</sup> based on the performance when calculating <sup>15</sup>N chemical shifts. The structures employed for **2a**, **4a**, and **5a** were fully optimized at the SCS-MP2/cc-pVTZ level of theory. The chemical shifts of **2a** were computed with reference to the experimental values of boron trichloride (<sup>11</sup>B 46.5 ppm) and 4-fluoroaniline (<sup>19</sup>F -127.5 ppm, <sup>15</sup>N 51.7 ppm), and as a relative shift for **4a** vs. **5a**.

## Conflicts of interest

There are no conflicts to declare.

## Acknowledgements

M. K. and C. K. thank the Fonds der chemischen Industrie for fellowships. We thank Dr Klaus Eichele for the measurement and interpretation of the solid state <sup>11</sup>B NMR spectra. The computations were performed on the BwForCluster JUSTUS. The authors acknowledge support from the state of Baden-Württemberg through bwHPC and the German Research Foundation (DFG) through grant no. INST 40/467-1 FUGG.

## References

- Q. Zeng, H. Wang, W. Fu, Y. Gong, W. Zhou, P. M. Ajayan, J. Lou and Z. Liu, *Small*, 2014, **11**, 1868–1884.
- L. Ci, L. Song, C. Jin, D. Jariwala, D. Wu, Y. Li, A. Srivastava, Z. F. Wang, K. Storr, L. Balicas, F. Liu and P. M. Ajayan, *Nat. Mater.*, 2010, **9**, 430–435.
- Y. Zheng, Y. Jiao, L. Ge, M. Jaroniec and S. Z. Qiao, *Angew. Chem., Int. Ed.*, 2013, **52**, 3110–3116.
- B. Muchharla, A. Pathak, Z. Liu, L. Song, T. Jayasekera, S. Kar, R. Vajtai, L. Balicas, P. M. Ajayan, S. Talapatra and N. Ali, *Nano Lett.*, 2013, **13**, 3476–3481.
- Z. Liu, L. Ma, G. Shi, W. Zhou, Y. Gong, S. Lei, X. Yang, J. Zhang, J. Yu, K. P. Hackenberg, A. Babakhani, J.-C. Idrobo, R. Vajtai, J. Lou and P. M. Ajayan, *Nat. Nanotechnol.*, 2013, **8**, 119–124.
- Y. Gong, G. Shi, Z. Zhang, W. Zhou, J. Jung, W. Gao, L. Ma, Y. Yang, S. Yang, G. You, R. Vajtai, Q. Xu, A. H. MacDonald, B. I. Yakobson, J. Lou, Z. Liu and P. M. Ajayan, *Nat. Nanotechnol.*, 2014, **5**, 3193.
- S. Beniwal, J. Hooper, D. P. Miller, P. S. Costa, G. Chen, S.-Y. Liu, P. A. Dowben, E. C. H. Sykes, E. Zurek and A. Enders, *ACS Nano*, 2017, **11**, 2486–2493.
- Z.-S. Wu, A. Winter, L. Chen, Y. Sun, A. Turchanin, X. Feng and K. Müllen, *Adv. Mater.*, 2012, **24**, 5130–5135.
- X.-Y. Wang, J.-Y. Wang and J. Pei, *Chem. – Eur. J.*, 2015, **21**, 3528–3539.
- M. M. Morgan and W. E. Piers, *Dalton Trans.*, 2016, **45**, 5920–5924.
- D. Bonifazi, F. Fasano, M. M. Lorenzo-Garcia, D. Marinelli, H. Oubaha and J. Tasseroul, *Chem. Commun.*, 2015, **51**, 15222–15236.
- N. Kalashnyk, P. Ganesh Nagaswaran, S. Kervyn, M. Riello, B. Moreton, T. S. Jones, A. De Vita, D. Bonifazi and G. Costantini, *Chem. – Eur. J.*, 2014, **20**, 11856–11862.
- X. Wang, F. Zhang, K. S. Schellhammer, P. Machata, F. Ortmann, G. Cuniberti, Y. Fu, J. Hunger, R. Tang, A. A. Popov, R. Berger, K. Müllen and X. Feng, *J. Am. Chem. Soc.*, 2016, **138**, 11606–11615.
- C. Sánchez-Sánchez, S. Brüller, H. Sachdev, K. Müllen, M. Krieg, H. F. Bettinger, A. Nicolai, V. Meunier, L. Talirz, R. Fasel and P. Ruffieux, *ACS Nano*, 2015, **9**, 9228–9235.
- X.-Y. Wang, F.-D. Zhuang, R.-B. Wang, X.-C. Wang, X.-Y. Cao, J.-Y. Wang and J. Pei, *J. Am. Chem. Soc.*, 2014, **136**, 3764–3767.
- M. Krieg, F. Reicherter, P. Haiss, M. Ströbele, K. Eichele, M.-J. Treanor, R. Schaub and H. F. Bettinger, *Angew. Chem., Int. Ed.*, 2015, **54**, 8284–8286.
- M. Fingerle, C. Maichle-Mössmer, S. Schundelmeier, B. Speiser and H. F. Bettinger, *Org. Lett.*, 2017, **19**, 4428–4431.
- J. Dosso, J. Tasseroul, F. Fasano, D. Marinelli, N. Biot, A. Fermi and D. Bonifazi, *Angew. Chem., Int. Ed.*, 2017, **56**, 4483–4487.
- B. Neue, J. F. Araneda, W. E. Piers and M. Parvez, *Angew. Chem., Int. Ed.*, 2013, **52**, 9966–9969.
- H. Helten, *Chem. – Eur. J.*, 2016, **22**, 12972–12982.
- H. Wei, Y. Liu, T. Y. Gopalakrishna, H. Phan, X. Huang, L. Bao, J. Guo, J. Zhou, S. Luo, J. Wu and Z. Zeng, *J. Am. Chem. Soc.*, 2017, **139**, 15760–15767.

- 22 M. Numano, N. Nagami, S. Nakatsuka, T. Katayama, K. Nakajima, S. Tatsumi, N. Yasuda and T. Hatakeyama, *Chem. – Eur. J.*, 2016, **22**, 11574–11577.
- 23 M. Stępień, E. Gońka, M. Żyła and N. Sprutta, *Chem. Rev.*, 2016, **117**, 3479–3716.
- 24 T. Wu, H. Shen, L. Sun, B. Cheng, B. Liu and J. Shen, *New J. Chem.*, 2012, **36**, 1385–1391.
- 25 C.-K. Chang, S. Kataria, C.-C. Kuo, A. Ganguly, B.-Y. Wang, J.-Y. Hwang, K.-J. Huang, W.-H. Yang, S.-B. Wang, C.-H. Chuang, M. Chen, C.-I. Huang, W.-F. Pong, K.-J. Song, S.-J. Chang, J.-H. Guo, Y. Tai, M. Tsujimoto, S. Isoda, C.-W. Chen, L.-C. Chen and K.-H. Chen, *ACS Nano*, 2013, **7**, 1333–1341.
- 26 G. H. Han, J. A. Rodríguez-Manzo, C.-W. Lee, N. J. Kybert, M. B. Lerner, Z. J. Qi, E. N. Dattoli, A. M. Rappe, M. Drndic and A. T. C. Johnson, *ACS Nano*, 2013, **7**, 10129–10138.
- 27 G. Imamura, C. W. Chang, Y. Nabae, M.-A. Kakimoto, S. Miyata and K. Saiki, *J. Phys. Chem. C*, 2012, **116**, 16305–16310.
- 28 A. Stock and E. Pohland, *Ber. Dtsch. Chem. Ges. A/B*, 1926, **59**, 2215–2223.
- 29 S. J. Groszos and S. F. Stafiej, *J. Am. Chem. Soc.*, 1958, **80**, 1357–1360.
- 30 H. S. Turner and R. J. Warne, *J. Chem. Soc.*, 1965, 6421–6450.
- 31 S. Rideal, *Ber. Dtsch. Chem. Ges.*, 1889, **22**, 992–993.
- 32 R. G. Jones and C. R. Kinney, *J. Am. Chem. Soc.*, 1939, **61**, 1378–1381.
- 33 C. A. Brown and A. W. Laubengayer, *J. Am. Chem. Soc.*, 1955, **77**, 3699–3700.
- 34 H. Nöth and H. Sachdev, *Z. Naturforsch.*, 1997, **52b**, 1345–1348.
- 35 I. M. Butcher and W. Gerrard, *J. Inorg. Nucl. Chem.*, 1965, **27**, 823–829.
- 36 S. Kervyn, O. Fenwick, F. D. Stasio, Y. S. Shin, J. Wouters, G. Accorsi, S. Osella, D. Beljonne, F. Cacialli and D. Bonifazi, *Chem. – Eur. J.*, 2013, **19**, 7771–7779.
- 37 A. Wakamiya, T. Ide and S. Yamaguchi, *J. Am. Chem. Soc.*, 2005, **127**, 14859–14866.
- 38 R. K. Bartlett, H. S. Turner, R. J. Warne, M. A. Young and I. J. Lawrenson, *J. Chem. Soc. A*, 1966, 479–500.
- 39 W. Gerrard and E. F. Mooney, *J. Chem. Soc.*, 1960, 4028–4036.
- 40 I. B. Atkinson, D. B. Clapp, C. A. Beck and B. R. Currell, *J. Chem. Soc., Dalton Trans.*, 1972, 182–185.
- 41 C. T. Kwon and H. A. McGee, *Inorg. Chem.*, 1973, **12**, 696–697.
- 42 G. A. Kapralova, T. V. Suchkova and A. M. Chaikin, *Mendeleev Commun.*, 1993, **3**, 118–120.
- 43 A. H. McDaniel and M. D. Allendorf, *J. Phys. Chem. A*, 1998, **102**, 7804–7812.
- 44 M. D. Allendorf and C. F. Melius, *J. Phys. Chem. A*, 1997, **101**, 2670–2680.
- 45 S. Reinhardt, M. Gastreich and C. M. Marian, *Phys. Chem. Chem. Phys.*, 2000, **2**, 955–963.
- 46 R. L. Hunt and B. S. Ault, *Spectrosc. Int. J.*, 1982, **1**, 31–44.
- 47 A. G. Avent, P. B. Hitchcock, M. F. Lappert, D.-S. Liu, G. Mignani, C. Richard and E. Roche, *J. Chem. Soc., Chem. Commun.*, 1995, 855–856.
- 48 *CRC Handbook of Chemistry and Physics*, ed. D. R. Lide, CRC Press, 2003–2004.
- 49 J. R. Blackborow and J. C. Lockhart, *J. Chem. Soc. A*, 1969, 816–819.
- 50 J. R. Blackborow, J. E. Blackmore and J. C. Lockhart, *J. Chem. Soc. A*, 1971, 49–53.
- 51 C. Spencer and W. N. Lipscomb, *J. Chem. Phys.*, 1958, **28**, 355.
- 52 A. C. Testa, *Spectrochim. Acta, Part A*, 1999, **55**, 299–309.
- 53 W. A. Burns and K. R. Leopold, *J. Am. Chem. Soc.*, 1993, **115**, 11622–11623.
- 54 U. Braun, T. Haberer, H. Nöth, H. Piotrowski and M. Warchhold, *Eur. J. Inorg. Chem.*, 2002, 1132–1145.
- 55 W. H. Press, S. A. Teukolsky, W. T. Vetterling and B. P. Flannery, *Numerical Recipes - The Art of Scientific Computing*, Cambridge University Press, 3rd edn, 2007.
- 56 W. Gerrard, H. R. Hudson and E. F. Mooney, *J. Chem. Soc.*, 1960, 5168–5172.
- 57 E. Wiberg and A. Bolz, *Ber. Dtsch. Chem. Ges. B*, 1940, **73B**, 209–232.
- 58 E. Wiberg and K. Hertwig, *Z. Anorg. Chem.*, 1947, **255**, 141–184.
- 59 E. Wiberg, K. Hertwig and A. Bolz, *Z. Anorg. Chem.*, 1948, **256**, 177–216.
- 60 E. Wiberg and K. Hertwig, *Z. Anorg. Chem.*, 1948, **257**, 138–144.
- 61 C. A. Jaska, K. Temple, A. J. Lough and I. Manners, *J. Am. Chem. Soc.*, 2003, **125**, 9424–9434.
- 62 Y. Kawano, M. Uruichi, M. Shimoi, S. Taki, T. Kawaguchi, T. Kakizawa and H. Ogino, *J. Am. Chem. Soc.*, 2009, **131**, 14946–14957.
- 63 H. Helten, A. P. M. Robertson, A. Staubitz, J. R. Vance, M. F. Haddow and I. Manners, *Chem. – Eur. J.*, 2012, **18**, 4665–4680.
- 64 G. R. Fulmer, A. J. M. Miller, N. H. Sherden, H. E. Gottlieb, A. Nudelman, B. M. Stoltz, J. E. Bercaw and K. I. Goldberg, *Organometallics*, 2010, **29**, 2176–2179.
- 65 K. Eichele, *WSolids1, version 1.20.21*, 2013.
- 66 *BrukerBioSpin, Topspin, V2.1*, Bruker BioSpin, 2009.
- 67 *APEX II, v2012.10-0*, Bruker AXS, Inc., Madison, WI, USA, 2012.
- 68 G. M. Sheldrick, *SADABS, 2012/1*, Bruker AXS Inc., Madison, WI, USA, 2012.
- 69 G. Sheldrick, *Acta Crystallogr., Sect. C: Struct. Chem.*, 2015, **71**, 3–8.
- 70 C. B. Hübschle, G. M. Sheldrick and B. Dittrich, *J. Appl. Crystallogr.*, 2011, **44**, 1281–1284.
- 71 S. Grimme, *J. Chem. Phys.*, 2003, **118**, 9095–9102.
- 72 S. Grimme, L. Goerigk and R. F. Fink, *Wiley Interdiscip. Rev.: Comput. Mol. Sci.*, 2012, **2**, 886–906.
- 73 F. Weigend and M. Häser, *Theor. Chem. Acc.*, 1997, **97**, 331–340.
- 74 T. H. Dunning, *J. Chem. Phys.*, 1989, **90**, 1007–1023.

- 75 F. Weigend, A. Köhn and C. Hättig, *J. Chem. Phys.*, 2002, **116**, 3175–3183.
- 76 Y. Zhao and D. Truhlar, *Theor. Chem. Acc.*, 2008, **120**, 215–241.
- 77 R. Krishnan, J. S. Binkley, R. Seeger and J. A. Pople, *J. Chem. Phys.*, 1980, **72**, 650–654.
- 78 M. J. Frisch, G. W. Trucks, H. B. Schlegel, G. E. Scuseria, M. A. Robb, J. R. Cheeseman, G. Scalmani, V. Barone, B. Mennucci, G. A. Petersson, H. Nakatsuji, M. Caricato, X. Li, H. P. Hratchian, A. F. Izmaylov, J. Bloino, G. Zheng, J. L. Sonnenberg, M. Hada, M. Ehara, K. Toyota, R. Fukuda, J. Hasegawa, M. Ishida, T. Nakajima, Y. Honda, O. Kitao, H. Nakai, T. Vreven, J. A. Montgomery, J. E. Peralta, F. Ogliaro, M. Bearpark, J. J. Heyd, E. Brothers, K. N. Kudin, V. N. Staroverov, R. Kobayashi, J. Normand, K. Raghavachari, A. Rendell, J. C. Burant, S. S. Iyengar, J. Tomasi, M. Cossi, N. Rega, J. M. Millam, M. Klene, J. E. Knox, J. B. Cross, V. Bakken, C. Adamo, J. Jaramillo, R. Gomperts, R. E. Stratmann, O. Yazyev, A. J. Austin, R. Cammi, C. Pomelli, J. W. Ochterski, R. L. Martin, K. Morokuma, V. G. Zakrzewski, G. A. Voth, P. Salvador, J. J. Dannenberg, S. Dapprich, A. D. Daniels, Ö. Farkas, J. B. Foresman, J. V. Ortiz, J. Cioslowski and D. J. Fox, *Gaussian 09, Revision D.01*, Gaussian, Inc., Wallingford CT, 2009.
- 79 C. Hättig, A. Hellweg and A. Kohn, *Phys. Chem. Chem. Phys.*, 2006, **8**, 1159–1169.
- 80 K. Raghavachari, G. W. Trucks, J. A. Pople and M. Head-Gordon, *Chem. Phys. Lett.*, 1989, **157**, 479.
- 81 TURBOMOLE V6.5 2012, a development of University of Karlsruhe and Forschungszentrum Karlsruhe GmbH, 1989–2007, TURBOMOLE GmbH, since 2007; available from <http://www.turbomole.com>.
- 82 K. Aidas, C. Angeli, K. L. Bak, V. Bakken, R. Bast, L. Boman, O. Christiansen, R. Cimiraglia, S. Coriani, P. Dahle, E. K. Dalskov, U. Ekström, T. Enevoldsen, J. J. Eriksen, P. Ettenhuber, B. Fernández, L. Ferrighi, H. Fliegl, L. Frediani, K. Hald, A. Halkier, C. Hättig, H. Heiberg, T. Helgaker, A. C. Hennum, H. Hettema, E. Hjertenæs, S. Høst, I.-M. Høyvik, M. F. Iozzi, B. Jansik, H. J. A. Jensen, D. Jonsson, P. Jørgensen, J. Kauczor, S. Kirpekar, T. Kjærgaard, W. Klopper, S. Knecht, R. Kobayashi, H. Koch, J. Kongsted, A. Krapp, K. Kristensen, A. Ligabue, O. B. Lutnæs, J. I. Melo, K. V. Mikkelsen, R. H. Myhre, C. Neiss, C. B. Nielsen, P. Norman, J. Olsen, J. M. H. Olsen, A. Osted, M. J. Packer, F. Pawłowski, T. B. Pedersen, P. F. Provasi, S. Reine, Z. Rinkevicius, T. A. Ruden, K. Ruud, V. V. Rybkin, P. Sałek, C. C. M. Samson, A. S. de Merás, T. Saue, S. P. A. Sauer, B. Schimmelpfennig, K. Snegov, A. H. Steindal, K. O. Sylvester-Hvid, P. R. Taylor, A. M. Teale, E. I. Tellgren, D. P. Tew, A. J. Thorvaldsen, L. Thøgersen, O. Vahtras, M. A. Watson, D. J. D. Wilson, M. Ziolkowski and H. Ågren, *Wiley Interdiscip. Rev.: Comput. Mol. Sci.*, 2014, **4**, 269–284.
- 83 *Dalton, a Molecular Electronic Structure Program, Release Dalton2016.2*, 2016, see <http://daltonprogram.org>.
- 84 T. W. Keal and D. J. Tozer, *J. Chem. Phys.*, 2004, **121**, 5654–5660.
- 85 F. Jensen, *J. Chem. Theory Comput.*, 2008, **4**, 719–727.
- 86 L. B. Krivdin, *Prog. Nucl. Magn. Reson. Spectrosc.*, 2017, **102–103**, 98–119.